

## Characterization and Antibacterial Activity Assessment of Hydroxyapatite-Betel Leaf Extract Formulation against *Streptococcus mutans* *In Vitro* and *In Vivo*

Fitriari Izzatunnisa Muhaimin<sup>1\*</sup>, Sari Edi Cahyaningrum<sup>2</sup>,  
Riska Amalia Lawarti<sup>2</sup>, and Dina Kartika Maharani<sup>2</sup>

<sup>1</sup>Department of Biology, Faculty of Science and Mathematics, Universitas Negeri Surabaya,  
Jl. Ketintang, Surabaya 60231, Indonesia

<sup>2</sup>Department of Chemistry, Faculty of Science and Mathematics, Universitas Negeri Surabaya,  
Jl. Ketintang, Surabaya 60231, Indonesia

\* **Corresponding author:**

email: fitriarimuhaimin@unesa.ac.id

Received: September 19, 2022

Accepted: December 15, 2022

DOI: 10.22146/ijc.77853

**Abstract:** Hydroxyapatite is an inorganic material that is commonly used as a remineralizing agent. Adding natural ingredients such as green betel leaf can increase the antibacterial properties due to the presence of phenolic compounds, flavonoids, and tannins. This study aims to determine the physical and chemical characteristics of the formulation of hydroxyapatite-betel leaf extract and the antibacterial activity against *Streptococcus mutans*. To characterize the combination of hydroxyapatite-betel leaf extract, XRD, PSA and FTIR analyses were performed. Particle size analysis showed the smallest results in the variation of betel 0.3 g, which is 690.08 nm. FTIR characterization showed the presence of OH, PO<sub>4</sub><sup>3-</sup> and CO<sub>3</sub><sup>2-</sup> functional groups from hydroxyapatite and C=O derived from betel leaf extract. In addition, *in vitro* and *in vivo* analyses were performed to assess the antibacterial activity of this formulation. The *in vitro* antibacterial activity test against *S. mutans* showed strong inhibitory activity. Our finding suggests that the formulation has the potential to be used as a medication or prevention agent for dental caries.

**Keywords:** hydroxyapatite; betel leaf; *Streptococcus mutans*

### ■ INTRODUCTION

Dental caries is one of the most common oral health problems in society which is caused by the interaction between teeth, microbial biofilms, and acids from food residues [1]. Another cause of dental caries is the formation of plaque on the teeth, a structured and organized multi-species biofilm caused by the presence of complex microbes that grow, survive, and colonize the tooth surface, such as *Streptococcus mutans* [2-5]. *S. mutans* bacteria play a role in synthesizing extracellular polymers of glucan from glucose by releasing glucosyltransferase to produce glucan from sucrose [6]. Glucans can promote the development of tooth surface biofilms by acting as binding intermediaries for other oral bacteria [7]. One of the factors that can increase the glucan synthesis ability of *S. mutans* is the sucrose-

dependent adhesion which causes the formation of plaque ecology and triggers dental caries [8]. Caries prevention can be done in various ways, one of which is the application of hydroxyapatite (HAp) as a remineralization agent [9].

HAp is the main inorganic mineral of bones and teeth with the shape of calcium phosphate crystals [10]. HAp is widely used in the medical field because of its biocompatibility, bioactivity, osteoconductivity, non-toxic, and non-immunogenic properties [11-12]. HAp can assist in the remineralization process of teeth, especially in dental caries caused by *S. mutans* bacteria, by acting as a source of calcium and phosphate ions [13]. Precursors that can be used to synthesize HAp include eggshells, clamshells, limestone, and beef bones [14-17].

Betel leaves (*Piper betle* L.) is a glabrous climbing vine that belongs to the *Piperaceae* family and can be

found in countries throughout Asia. It has been used for thousands of years in traditional medicine as a stimulant, antifungal, antioxidant, and antimicrobial agent due to its high phytochemical concentration [18]. Furthermore, it has bioactivity potential due to metabolite compounds such as phenols, flavonoids, and tannins that act as antibacterial agents [19]. A previous study has shown that betel leaf extract can inhibit gram-positive bacteria *Staphylococcus aureus* and gram-negative bacteria *Pseudomonas aeruginosa* [20]. Combining HAp with betel leaf extract can significantly increase antibacterial and antimicrobial properties against *S. aureus* [21].

In this study, we aim to determine the physical and chemical characteristics of the HAp-betel leaf extract formulation and its antibacterial activity against *S. mutans in vitro*. To address this, a formulation of HAp-betel leaf extract in liquid and gel preparations was carried out, which is expected to prevent tooth decay without any toxic effects.

## ■ EXPERIMENTAL SECTION

### Materials

Green betel leaves (*Piper betle* L.) were obtained from the Jombang area. Phosphoric acid (85%  $H_3PO_4$ ) and aquadest were purchased from PT. Brataco. Hydroxyapatite was synthesized from beef bone, according to [22]. Propylene glycol, NA, and NB medium were purchased from Merck, while gentamicin, saline, and Na-CMC were from PT. Gunacipta Multirasa. *Streptococcus mutans* (ATCC 35668) bacteria used in *in vitro* study were performed from the Microbiology Lab, Faculty of Medicine, Airlangga University. Winstar rats (*Rattus norvegicus*) used in *in vivo* study were performed by the Faculty of Veterinary, Airlangga University.

### Instrumentation

The functional groups of liquid and gel samples were analyzed using a Perkin-Elmer Spectrum Two™ IR spectrometer for frequencies ranging from 400 to 4000  $cm^{-1}$ . The particle size analysis of the formulations was analyzed using the Zetasizer Malvern series particle size analyzer. The diameter of the inhibition zone for the antibacterial activity test was measured using a digital

caliper with the Sigmat Vernier Caliper with an accuracy of  $\pm 0.2$  mm.

### Procedure

#### Hydroxyapatite synthesis-green betel leaf extract

The thick extract of green betel leaf obtained from the maceration of fresh green betel leaf with distilled water was weighed as much as 0.1; 0.3; 0.5; 0.7; and 1 g. Then put into a beaker, added 2 mL of 1% HAp solution made of 0.2 g of HAp dissolved in 20 mL of  $H_3PO_4$  and stirred until homogeneous [22]. The functional groups of liquid and gel samples were analyzed using a IR spectrometer.

#### Hydroxyapatite gel-green betel leaf extract

A total of 30 mL of distilled water was put into a beaker and then heated at 100 °C on a stirrer until it boiled. Then, 5 mL of propylene glycol and 50 mL mixture of HAp-green betel leaf extract were then added while stirring with a magnetic stirrer. In order to form gel consistency, 0.4 g of Na-CMC was stirred with a magnetic stirrer while heated [23]. X-Ray Diffraction (XRD) analysis was performed using the XRD Phillips PW-1170 Diffractometer ( $Cu-K\alpha = 1.5404 \text{ \AA}$ ). Next, particle size analysis of the formulations was analyzed using the Zetasizer Malvern series particle size analyzer. The material in the form of powder is weighed approximately 0.01 g then put into the beaker and mixed with 1 mL dispersant (Tween 20) while stirring thoroughly. Aquadest was added up to 10 mL and stirred until dissolved. Next, the sample was ultrasonicated for 5 s, put into a 1 mL cuvette then measured in diameter distribution using PSA.

#### Anti-bacterial activity test

Antibacterial activity was tested by the disc diffusion method. NA medium (Merck) was heated by autoclaving for 15 min at 120 °C. Next, 1 mL of suspension of *S. mutans* bacteria was taken, which had been inoculated on NB media (Merck) under sterile conditions and put into a petri dish. Solid media were made by pouring 5 mL of NA medium under slightly hot conditions into the petri dish. Furthermore, the petri dish is shaken slowly until the suspension of *S. mutans* bacteria, and NA media is homogeneous. Liquid and gel

formulation of HAp-green betel leaf extract with variations in the composition of green betel leaf extract 0.1; 0.3; 0.5; 0.7; and 1 g, positive control, negative control and blank dish was prepared. Next, the blank dish is dipped into the sample to be tested. Then put 3 blank dishes that had been dipped in samples into a petri dish containing NA media and *S. mutans* bacteria which started to solidify. Samples were then incubated at 37 °C for 24 h. After incubation, the petri dish was removed from the incubator, and the clear zone around the blank dish was measured using a digital caliper (Sigmat Vernier Caliper) [24]. The diameter of the inhibition zone for the antibacterial activity test was measured using a digital caliper with the Sigmat Vernier Caliper with an accuracy of  $\pm 0.2$  mm.

#### **Spreadability test**

A total of 0.5 g of HAp gel formulation-betel leaf extract was placed in the center of the glass and then covered with another glass. The measurement of dispersion is based on the diameter of the distribution of the preparation horizontally and vertically, with the addition of a load of 50 g to a total weight of 150 g [25].

#### **Adhesion test**

A total of 0.25 g of the HAp-betel leaf extract gel formulation was placed on a glass slide and then covered with another glass slide until it was completely covered. Next, a load weighing 1000 g is placed on top of the slide for 5 min. To remove the glass object from the gel attachment, a load weighing 80 g is used. The time needed for two glass slides is separated [26].

#### **In vivo testing on rats**

**Rats.** Male Wistar rats aged 10 weeks with an average weight of 150–200 g were used as experimental animals. The rats have received an animal certificate from the Animal Husbandry Service and were handled in accordance with the care guidelines of an *in vivo* ethical clearance research issued by the Faculty of Medicine, Universitas Airlangga (Decision no: 262/EC/KEPK/FKUA/2021). Rats were placed in polypropylene cages at a controlled temperature of  $25 \pm 5$  °C and were acclimatized for 7 days before the experiment was carried out [27].

#### **Test animal treatment**

A total of 9 male Wistar rats were divided into 3 groups, each consisting of 3 rats. Each group of Wistar rats was infected with 0.1 mL ( $10^6$  cfu/mL) of *S. mutans* suspension intraperitoneally. After 24 h, rats were injected with the positive control, negative control, and formulation of HAp gel-green betel leaf extract in each group. The positive control group was injected with 0.1 mL of gentamicin, while the negative control group was injected with 0.4 mL of saline solution. The treatment group was injected with 1 mL of HAp-green betel leaf extract via intraperitoneal. The injection was done intraperitoneally for 3 d. After 24 h, the specimen was removed from the intraperitoneal fluid. Then the intraperitoneal was diluted using NaCl to  $10^4$  cfu/mL to be tested for its antibacterial activity [28]. Next, 1 mL of diluted intraperitoneal fluid was cultured on NA media with the pouring agar method into a sterile petri dish and then added 15 mL of NA agar medium at 40–45 °C. After it solidified, plates were incubated at 37 °C for 24 h. Then, bacterial colonies were counted using the total plate count (TPC) method [24,29].

## **RESULTS AND DISCUSSION**

### **Hydroxyapatite-Betel Leaf Extract Formulation Characterization**

HAp-betel leaf extract formulation is characterized by conducting several analyses, such as XRD, PSA, and FTIR. To determine the physical characteristics, including chemical composition, crystallographic structure, and physical properties, XRD was performed. The results analysis shows that HAp calcined from bovine bones has similarities with HAp from the Tissue Bank, which has been applied in the medical field at Dr. Soetomo Hospital. Both HAp are dominated by the HAp phase, with the highest peak being at an angle of  $2\theta = 31.8023^\circ$ , which corresponds to JCPDS data number 09-0432. HAp ( $\text{Ca}_{10}(\text{PO}_4)_6(\text{OH})_2$ ) appears with a relative intensity of 100% (Fig. 1). Other phases formed in the two HAp are A-type carbonate apatite (AKA) and B-type carbonate apatite (AKB). AKA ( $\text{Ca}_{10}(\text{PO}_4)_6\text{CO}_3$ ) is formed because carbonate ions replace  $\text{OH}^-$  ions in the HAp structure, while AKB

(Ca<sub>10</sub>(PO<sub>4</sub>)<sub>3</sub>(CO<sub>3</sub>)(OH)<sub>2</sub>) is formed because carbonate ions replace PO<sub>4</sub><sup>3-</sup> ions in the HAp structure. AKA appears at an angle of  $2\theta = 26.0214^\circ$  and  $32.2708^\circ$  corresponding to JCPDS data number 35-0180. AKA appeared with relative intensities of 40.69 and 63.24%, respectively. AKB appears at  $2\theta = 28.234^\circ$ ; this corresponds to JCPDS data number 19-0272. AKB appeared with a relative intensity of 7.54%. In this study, the AKA phase is more dominant when compared to the AKB phase because HAp compounds are produced from the calcination process at high temperatures, namely 900 °C. However, if the synthesis of HAp is carried out at low temperatures (60–100 °C), the AKB phase will dominate more. A combination of carbonates is not harmful because it is also found in human bones as carbonate apatite [30].

To determine the particle size and distribution of liquid and gel formulations of HAp-green betel leaf extract samples, PSA was conducted. The results show the average particle size in the variation of the addition of betel extract are 0.1; 0.3; 0.5; 0.7; and 1 g are 5956.00; 690.08; 306300; 5042.40; and 5832.20 nm, respectively (Fig. 2).

Based on the results, the formulation of HAp and green betel leaf extract with 0.3 g of betel can be categorized in the nanoparticle group, while the variation of betel extract is 0.1, 0.5, 0.7, and 1 g is excluded. Nanoparticles are materials with a particle size of less than 1 μm [31]. Variations that have not been optimal in nano size are probably due to particle agglomeration. Thus, the particles grow bigger and easily detached. The larger the particle size, the greater the polarity and affinity [32]. The smaller the particle size, the larger the surface area, allowing for higher contact with microorganisms' cell walls [33]. Therefore, based on our results, further optimization is needed to prevent the agglomeration of HAp.

The determination of the functional groups in the sample was qualitatively analyzed using FTIR. Previously, we analyzed HAp calcined from bovine bones compared to HAp from the Tissue Bank. It can be seen that HAp calcined from bovine bones is similar to HAp from the Tissue Bank; this is evidenced by the typical functional

groups belonging to HAp that appear at almost the same wavenumber (Fig. 3(a1)). HAp from the analyzed bovine bone showed an absorption band of the OH<sup>-</sup> group at wavenumber 3572.68; 1993.09; and 602.51 cm<sup>-1</sup>, while HAp from the Network Bank showed absorption bands from the OH<sup>-</sup> group at wavenumber 3570.76; 2016.24; and 604.44 cm<sup>-1</sup>. It can be seen that the spectra of the OH<sup>-</sup> group look uncharacteristically pointed, which is seen to be this ramp because the OH<sup>-</sup> group of HAp binds to the metal Ca<sup>2+</sup> (Fig. 3(a2)). The PO<sub>4</sub><sup>3-</sup> the group

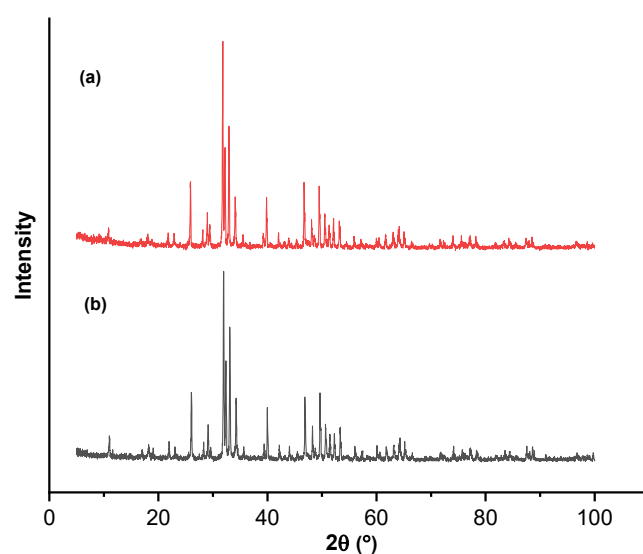


**Fig 1.** Results of the XRD spectrum (a) beef bone hydroxyapatite; (b) standard hydroxyapatite from the Tissue Bank (Dr. Soetomo Hospital)

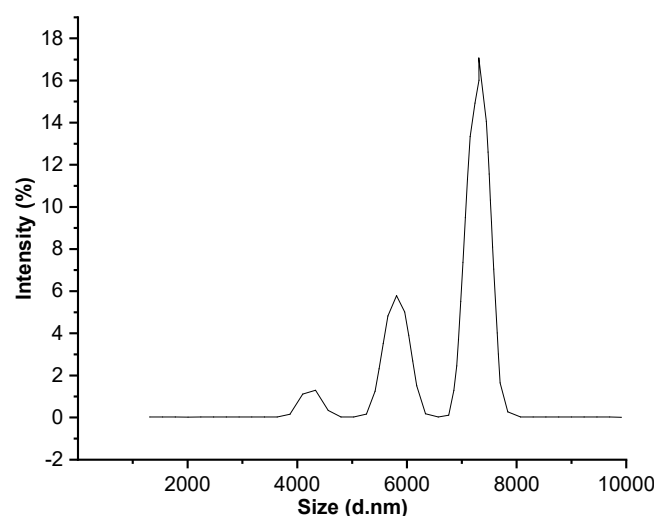


**Fig 2.** Graph of PSA analysis of the formulation of HAp-betel leaf extract

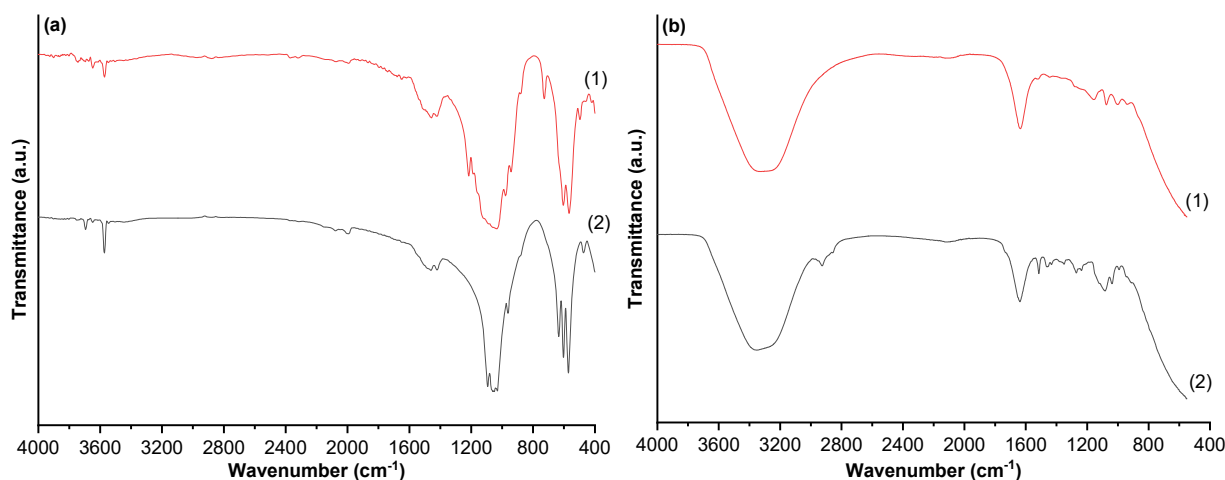


**Fig 3.** Results of the FTIR spectrum. (a) hydroxyapatite from beef bone (1) and Tissue bank (2); (b) HAp-betel leaf extract formulation in gel (1) and liquid sample (2)

has 4 vibration modes, namely stretching symmetry vibration ( $\nu_1$ ) with a wavenumber of about  $956\text{ cm}^{-1}$ , bending symmetry vibration ( $\nu_2$ ) with a wavenumber of about  $430\text{--}460\text{ cm}^{-1}$ , stretching asymmetry vibration ( $\nu_3$ ) with a wavenumber of about  $1040\text{--}1090\text{ cm}^{-1}$ , bending asymmetric vibration ( $\nu_4$ ) with a wavenumber of about  $571\text{--}610\text{ cm}^{-1}$ . Calcined HAp from bovine bones showed an absorption band of the carbonate group ( $\text{CO}_3^{2-}$ ) at a wavenumber of about  $1400\text{ cm}^{-1}$ . The presence of a carbonate group in the resulting HAp is caused by direct contact between HAp samples and carbon dioxide ( $\text{CO}_2$ ) in the air.

Meanwhile, the results of the FTIR analysis for the liquid sample (Fig. 3(b2)) showed peaks at a wavenumber of  $3325.44$ ,  $1634.72$ ,  $1156.81$ , and  $1075.29\text{ cm}^{-1}$  indicating the presence of a hydroxyl group (OH), a carbonyl group (C=O) and a carbonate group ( $\text{CO}_3^{2-}$ ) and a phosphate group ( $\text{PO}_4^{3-}$ ), respectively.

In the gel sample (Fig. 3(b1)), the hydroxyl (OH) group was detected at a wavenumber of  $3279.84\text{ cm}^{-1}$ , which was also previously observed by Liu et al. [34]. The carbonyl group (C=O) was seen at a wave of  $1639.49\text{ cm}^{-1}$ , indicating the presence of one of the functional groups of the metabolite compounds contained in the betel leaf. The carbonate group ( $\text{CO}_3^{2-}$ ) was detected at a wavenumber of  $1136.83\text{ cm}^{-1}$ . This finding is in line with the previous finding, which states that the carbonate group in human bone is detected at a wavenumber of  $\sim 1100.00\text{ cm}^{-1}$  [35].

The detected carbonate group comes from  $\text{CO}_2$  in the air, which reacts with calcium to form a bond so that a calcium carbonate phase appears during synthesis [36]. Furthermore, the phosphate group ( $\text{PO}_4^{3-}$ ) was detected at a wave of  $1078.69\text{ cm}^{-1}$ . Mondal et al. support the detection of phosphate groups, which states that wavenumbers between  $1000\text{--}1100\text{ cm}^{-1}$  indicate the presence of a phosphate group with a stretching vibration pattern [37].

The OH,  $\text{PO}_4^{3-}$  and  $\text{CO}_3^{2-}$  functional groups are functional groups derived from HAp, but the C=O group is a functional group derived from green betel leaf extract [38]. The existence of a shifting wavenumber indicates that there has been a bond between HAp and the metabolite compounds present in the green betel leaf extract (Table 1).

Next, the gel preparation spreadability test was carried out to determine the ability of the formulation of HAp-green betel leaf extract gel to spread when applied to the teeth (Table 2). Dispersibility is an important characteristic in formulations, as it affects the transfer of the active ingredient to the target area at the correct dose, ease of use, the pressure required to exit the package, and acceptance by the consumer. The dispersion is related to water; the more water content, the wider the dispersion [39]. The results of the tests showed that the increase in the spreading area was accompanied by adding a given load (Table 3). The formula found the best



**Table 1.** Wavenumber data from FTIR

Functional groups	HAp wavenumber (cm <sup>-1</sup> )			
	Beef bone	Tissue bank	Liquid sample	Gel sample
OH	604.44	602.51	3325.44	3279.84
	2016.24	1993.09	-	
	3570.76	3572.68	-	
C=O	-	-	1634.72	1639.49
CO <sub>3</sub> <sup>2-</sup>	1414.49	1420.27	1156.81	1136.83
	1462.70	1460.78		
PO <sub>4</sub> <sup>3-</sup>	961.25	961.25	1075.29	1078.69
	471.36	473.29		
	1048.04	1049.97		
	1090.47	1092.40		
	571.65	571.65		
	961.25	961.25		

**Table 2.** Test results of HAp gel-betel leaf extract spreadability

Sample	Horizontal (cm)	Vertical (cm)	Average
Betel 0.1 g	7.77	8.23	8.00
Betel 0.3 g	8.54	8.28	8.41
Betel 0.5 g	8.82	9.12	8.97
Betel 0.7 g	8.53	8.67	8.60
Betel 1 g	8.84	8.82	8.83

**Table 3.** The results of the stickiness test of the HAp gel-betel leaf extract

Sample	Adhesion (s)
Betel 0.1 g	1.83
Betel 0.3 g	1.03
Betel 0.5 g	0.78
Betel 0.7 g	1.07
Betel 1 g	0.88

results by adding 0.1 g of betel leaf because it has a spreading power close to the dispersion scale that meets the standards. Good dispersion will provide the speed of contact between the gel and the teeth. The viscosity value of the preparation influences the difference in dispersion. It has a low viscosity value (watery) which results in the dispersion diameter becoming large because it is easier to flow. While for preparations that have a high viscosity value, the resulting dispersion diameter is small [40]. Preparations that are too spread or difficult to spread will reduce the comfort and effectiveness of use, while

preparations that are too dilute will cause reduced adhesion. Therefore, the contact time of active substances with the application site will reduce [41]. Many factors affect the dispersion, one of which is the amount and strength of the gel matrix. The dispersion will decrease along with the more and the strength of the gel matrix. In this case, what affects the formation of the gel matrix is the gelling agent, therefore, the concentration of the gelling agent can increase and strengthen the gel matrix [42].

To determine the adhesion time of the hydroxyapatite gel formulation-green betel leaf extract to the tooth surface adhesive test was performed. Hence, it will suggest whether the active substances in the preparation were absorbed. The general characteristic of gel preparations is the ability to adhere to the surface of the application for a long time. The longer the preparation time can be attached, and the additive can be in contact with the application, the antibacterial effect is expected to be optimal [43]. The data suggest that the differences in the stickiness of each formulation are due to differences in the composition of the green betel leaf extract, which affects the viscosity and spreadability (Table 4). Adhesion to toothpaste is related to the absorption of the active substance into the teeth. Based on the tested samples, the formula with the addition of 0.1; 0.3; and 0.7 betel leaf extract meet the standard of adhesion test, which is above 1 s. Adhesion of semi-solid

**Table 4.** Inhibition zone of HAp-betel leaf extract formulation

Sample	Clear zone diameter (mm)			Average
Liquid betel 0.1 g	22.6	22.5	20.1	21.73 ± 9.58
Liquid betel 0.3 g	17.3	16.1	16.6	16.67 ± 14.27
Liquid betel 0.5 g	18.4	18.9	18.2	18.50 ± 8.39
Liquid betel 0.7 g	20.0	20.6	17.8	19.47 ± 11.22
Liquid betel 1 g	18.4	18.9	20.5	19.27 ± 2.19
Gel betel 0.1 g	12.7	12.6	11.2	12.17 ± 20.07
Gel betel 0.3 g	13.6	14.8	13.9	14.10 ± 14.59
Gel betel 0.5 g	9.2	7.7	10.6	9.17 ± 10.48
Gel betel 0.7 g	12.8	13.3	14.5	13.53 ± 20.58
Gel betel 1 g	12.7	13.6	12.6	12.97 ± 13.13
Hydroxyapatite	14.7	11.2	9.1	11.67 ± 19.53
Aquadest	0	0	0	0

preparations should be more than 1 s [42]. In addition, the addition of Na CMC in the gel system in excess can interfere with the ionization process of the carboxyl group.

#### **In Vitro Antibacterial Activity Test**

HAp is widely studied as an excellent candidate for bone repair and substitution. Recently, studies conducted by Seyedmajidi et al. [44] have shown that HAp has an antibacterial activity by killing *S. mutans* in different concentrations. In addition, another study has shown that the antimicrobial effect of piper betel leaf extract against *S. mutans* formulation can inhibit the growth of *S. mutans* [45]. To determine the antibacterial activity of HAp-betel leaf extract in liquid and gel formulation antibacterial activity test was conducted by disc diffusion method *in vitro*. The results showed the ability to inhibit the growth of *S. mutans*, as indicated by forming a clear zone around the colony (Fig. 4). The data obtained were analyzed by statistical tests, including a normality test, one-way ANOVA and a follow-up test using Duncan. One way ANOVA test with a confidence level of 5% obtained results with a significant level of 0.000 ( $p < 0.05$ ) so that it can be seen that there is a significant difference between one data and another. The normality test received a significant value of 0.200 ( $p > 0.05$ ), which indicates that the variety of inhibition zones in the HAp-green betel leaf extract formulation was normally distributed. Furthermore, Duncan's test was carried out as a follow-up test, which showed that the formulation of

HAp-green betel leaf extract had an inhibitory effect on *S. mutans*. The clear zone was categorized based on its diameter with a range below 5 mm as weak inhibition, 5–10 mm as moderate inhibition, 10–20 mm as strong inhibition, and above 20 mm have very strong resistance [38]. In liquid form, betel extract of 0.1 g has the most

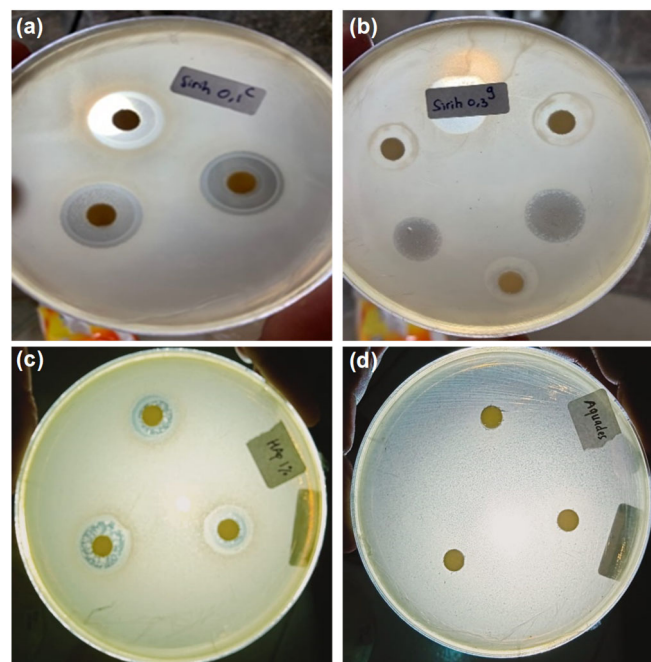


**Fig 4.** Clear zone formation of HAp-green betel extract against the growth of *S. mutans* in (a) Liquid formulation, (b) gel formulation, (c) 1% hydroxyapatite was used as a positive control, and (d) aquadest was used as a negative control

expansive clear zone with around 21.73 mm, while in gel form is 14.10 mm (Table 4). This observation indicates that the increasing concentration of betel leaf did not dictate the size of clear zone formation. The data suggests that there may be an optimum concentration of betel leaf that will give the best effects in the growth inhibition of *S. mutans*.

Overall, the formulation of HAp-green betel leaf extract has strong inhibition against *S. mutans* bacteria. It is caused by secondary metabolites activity of green betel leaves, such as phenols, flavonoids, and tannins that damage the bacterial cell membrane. Phenol compounds can denature bacterial cells by disrupting the covalent structure of gram-positive bacteria [46-47]. The presence of carboxyl groups in aromatic hydrocarbons will form complexes with extracellular proteins, which result in the loss of the infection ability of bacteria. Flavonoid compounds act as antibacterial agents that interfere with the potassium concentration of gram-positive bacteria, cause the malfunction of the cytoplasmic membrane and inhibit the adhesion and biofilm formation [48]. In addition, flavonoid compounds can cause damage to the phospholipid bilayer and inhibit the respiratory chain or ATP synthesis in gram-positive bacteria [49]. Tannins work by destroying bacterial cell membranes by inactivating the function of genetic material and inactivating enzymes. It will inhibit the growth of bacteria and inactivate the ability to stick to bacteria [50-51].

### In Vivo Antibacterial Activity Test

*In vivo* test was conducted to determine the antibacterial activity of the HAp formulation of green betel leaf extract against rats infected with *S. mutans*

bacteria. In this test, gentamicin was used as a positive control, saline as a negative control, and the sample was in the form of a gel formulation of HAp-betel leaf extract with variations in the addition of 0.3 g of betel leaf extract.

The results have shown that the number of colonies in the gel formulation was greater than that of the positive control and negative control (Fig. 5 and Table 5). This could be due to the long storage of the formulation and dilution needs to be conducted in order to get a better analysis of the colony counts. However, there were no toxic side effects to the rats after testing, and the rats were in good health.

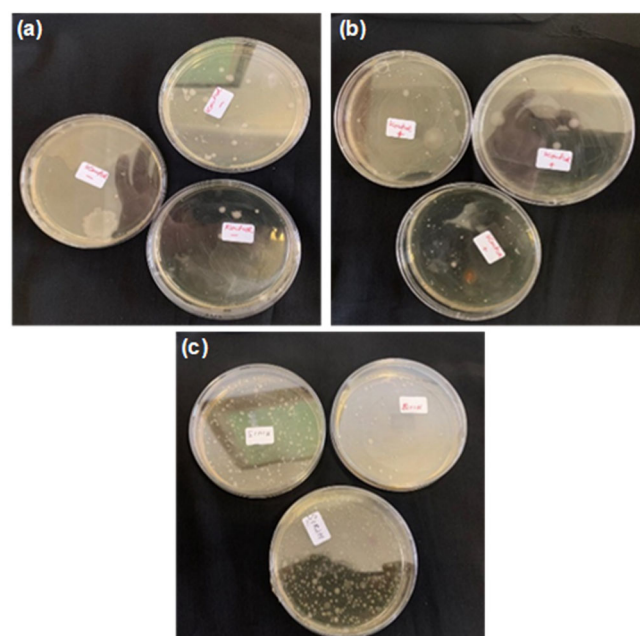


**Fig 5.** Colony test results (a) saline as negative controls; (b) gentamicin as positive controls; (c) hydroxyapatite gel formulation-green betel leaf extract

**Table 5.** Number of colonies after treatment on rats

Group	Number of colonies			Average
	Rat 1	Rat 2	Rat 3	
Saline (-)	167	96	70	111.00 ± 50.21
Gentamicin (+)	193	218	75	162.00 ± 76.37
Betel 0.3 g	313	421	260	331.33 ± 82.05

\*The data were normally distributed with a significant value of 0.200 ( $p > 0.05$ ). Then a one-way ANOVA test was performed with a significant level of 5%, and a significant value of 0.021 ( $p < 0.05$ ) was performed, which indicated that there was a difference from one data to another



## ■ CONCLUSION

Hydroxyapatite-betel leaf extract formulation characterization has shown there is a bond between hydroxyapatite and the metabolite compounds present in the green betel leaf extract. In addition, the spreadability of the formulation also already meets the standard of toothpaste. Antibacterial *in vitro* test suggests that a combination of hydroxyapatite and betel leaf extract gives high antibacterial activity against *S. mutans*. Unfortunately, our *in vivo* study failed to validate this due to the possibility of improper storage of the formulation. However, it was shown that there were no toxic effects of the formulation on the test animal, which indicates the safe formulation for caries prevention or treatment. Based on our results, the hydroxyapatite-betel leaf extract formulation has shown its high potential as an ingredient to prevent tooth decay and the observed concentration already meets the standard even though *in vivo* study needs to be repeated. Furthermore, the potential of this formulation can be explored further, especially in the demineralization potential with its hydroxyapatite composition.

## ■ ACKNOWLEDGMENTS

The authors would like to thank DIKTI for the financial support through research funding *Hibah Penelitian Terapan Unggulan Perguruan Tinggi* (PTUPT) program 2022 No. contract: B/29531/UN38.9/LK.0400/2022.

## ■ REFERENCES

- [1] Cho, G.J., Kim, S.Y., Lee, H.C., Kim, H.Y., Lee, K.M., Han, S.W., and Oh, M.J., 2020, Association between dental caries and adverse pregnancy outcomes, *Sci. Rep.*, 10 (1), 5309.
- [2] Gutiérrez-Venegas, G., Gómez-Mora, J.A., Meraz-Rodríguez, M.A., Flores-Sánchez, M.A., and Ortiz-Miranda, L.F., 2019, Effect of flavonoids on antimicrobial activity of microorganisms present in dental plaque, *Heliyon*, 5 (12), e03013.
- [3] Pitts, N.B., Twetman, S., Fisher, J., and Marsh, P.D., 2021, Understanding dental caries as a non-communicable disease, *Br. Dent. J.*, 231 (12), 749–753.
- [4] Gholibegloo, E., Karbasi, A., Pourhajibagher, M., Chiniforush, N., Ramazani, A., Akbari, T., Bahador, A., and Khoobi, M., 2018, Carnosine-graphene oxide conjugates decorated with hydroxyapatite as promising nanocarrier for ICG loading with enhanced antibacterial effects in photodynamic therapy against *Streptococcus mutans*, *J. Photochem. Photobiol., B*, 181, 14–22.
- [5] Chen, X., Daliri, E.B.M., Kim, N., Kim, J.R., Yoo, D., and Oh, D.H., 2020, Microbial etiology and prevention of dental caries: Exploiting natural products to inhibit cariogenic biofilms, *Pathogens*, 9 (7), 569.
- [6] Mallya, P.S., and Mallya, S., 2020, Microbiology and clinical implications of dental caries – A review, *J. Evol. Med. Dent. Sci.*, 9 (48), 3670–3675.
- [7] Watanabe, A., Kawada-Matsuo, M., Le, M.N.T., Hisatsune, J., Oogai, Y., Nakano, Y., Nakata, M., Miyawaki, S., Sugai, M., and Komatsuzawa, H., 2021, Comprehensive analysis of bacteriocins in *Streptococcus mutans*, *Sci. Rep.*, 11 (1), 12963.
- [8] Lemos, J.A., Palmer, S.R., Zeng, L., Wen, Z.T., Kajfasz, J.K., Freires, I.A., Abranches, J., and Brady, L.J., 2019, The Biology of *Streptococcus mutans*, *Microbiol. Spectrum*, 7 (1), 7.1.03.
- [9] Amaechi, B.T., Phillips, T.S., Evans, V., Ugwokaegbe, C.P., Luong, M.N., Okoye, L.O., Meyer, F., and Enax, J., 2021, The potential of hydroxyapatite toothpaste to prevent root caries: A pH-cycling study, *Clin., Cosmet. Invest. Dent.*, 13, 315–324.
- [10] Sawada, M., Sridhar, K., Kanda, Y., and Yamanaka, S., 2021, Pure hydroxyapatite synthesis originating from amorphous calcium carbonate, *Sci. Rep.*, 11 (1), 11546.
- [11] Suresh Kumar, C., Dhanaraj, K., Vimalathithan, R.M., Ilaiyaraja, P., and Suresh, G., 2020, Hydroxyapatite for bone related applications derived from sea shell waste by simple precipitation method, *J. Asian Ceram. Soc.*, 8 (2), 416–429.
- [12] Siddiqui, H.A., Pickering, K.L., and Mucalo, M.R., 2018, A review on the use of hydroxyapatite-carbonaceous structure composites in bone

- replacement materials for strengthening purposes, *Materials*, 11 (10), 1813.
- [13] Nozari, A., Ajami, S., Rafiei, A., and Niazi, E., 2017, Impact of nano hydroxyapatite, nano silver fluoride and sodium fluoride varnish on primary enamel remineralization: An *in vitro* study, *J. Clin. Diagn. Res.*, 11 (9), ZC97–ZC100.
- [14] Wu, S.C., Hsu, H.C., Hsu, S.K., Chang, Y.C., and Ho, W.F., 2016, Synthesis of hydroxyapatite from eggshell powders through ball milling and heat treatment, *J. Asian Ceram. Soc.*, 4 (1), 85–90.
- [15] Mtavangu, S.G., Mahene, W., Machunda, R.L., van der Bruggen, B., and Njau, K.N., 2022, Cockle (*Anadara granosa*) shells-based hydroxyapatite and its potential for defluoridation of drinking water, *Results Eng.*, 13, 100379.
- [16] Sinulingga, K., Sirait, M., Siregar, N., and Abdullah, H., 2021, Synthesis and characterizations of natural limestone-derived nano-hydroxyapatite (HAP): A comparison study of different metals doped HAPs on antibacterial activity, *RSC Adv.*, 11 (26), 15896–15904.
- [17] Manalu, J.L., Soegijono, B., and Indrani, D.J., 2015, Characterization of hydroxyapatite derived from bovine bone, *Asian J. Appl. Sci.*, 3 (4), 758–765.
- [18] Nayaka, N.M.D.M.W., Sasadara, M.M.V., Sanjaya, D.A., Yuda, P.E.S.K., Dewi, N.L.K.A.A., Cahyaningsih, E., and Hartati, R., 2021, *Piper betle* (L): Recent review of antibacterial and antifungal properties, safety profiles, and commercial applications, *Molecules*, 26 (8), 2321.
- [19] Lubis, R.R., Marlisa, M., and Wahyuni, D.D., 2020, Antibacterial activity of betle leaf (*Piper betle* L.) extract on inhibiting *Staphylococcus aureus* in conjunctivitis patient, *Am. J. Clin. Exp. Immunol.*, 9 (1), 1–5.
- [20] Madhumita, M., Guha, P., and Nag, A., 2019, Extraction of betel leaves (*Piper betle* L.) essential oil and its bio-actives identification: Process optimization, GC-MS analysis and anti-microbial activity, *Ind. Crops Prod.*, 138, 111578.
- [21] Umesh, M., Choudhury, D.D., Shanmugam, S., Ganesan, S., Alsehli, M., Elfasakhany, A., and Pugazhendhi, A., 2021, Eggshells biowaste for hydroxyapatite green synthesis using extract piper betel leaf - Evaluation of antibacterial and antibiofilm activity, *Environ. Res.*, 200, 111493.
- [22] Puzanov, I., Diab, A., Abdallah, K., Bingham, C.O., Brogdon, C., Dadu, R., Hamad, L., Kim, S., Lacouture, M.E., LeBoeuf, N.R., Lenihan, D., Onofrei, C., Shannon, V., Sharma, R., Silk, A.W., Skondra, D., Suarez-Almazor, M.E., Wang, Y., Wiley, K., Kaufman, H.L., Ernstoff, M.S., and Society for Immunotherapy of Cancer Toxicity Management Working Group, 2017, Managing toxicities associated with immune checkpoint inhibitors: Consensus recommendations from the Society for Immunotherapy of Cancer (SITC) Toxicity Management Working Group, *J. ImmunoTher. Cancer*, 5 (1), 95.
- [23] Qian, G., Liu, W., Zheng, L., and Liu, L., 2017, Facile synthesis of three dimensional porous hydroxyapatite using carboxymethylcellulose as a template, *Results Phys.*, 7, 1623–1627.
- [24] Hoelzer, K., Cummings, K.J., Warnick, L.D., Schukken, Y.H., Siler, J.D., Gröhn, Y.T., Davis, M.A., Besser, T.E., and Wiedmann, M., 2011, Agar disk diffusion and automated microbroth dilution produce similar antimicrobial susceptibility testing results for *Salmonella* serotypes Newport, Typhimurium, and 4,5,12:i-, but differ in economic cost, *Foodborne Pathog. Dis.*, 8 (12), 1281–1288.
- [25] Dantas, M.G.B., Reis, S.A.G.B., Damasceno, C.M.D., Rolim, L.A., Rolim-Neto, P.J., Carvalho, F.O., Quintans-Junior, L.J., and da Silva Almeida, J.R.G., 2016, Development and evaluation of stability of a gel formulation containing the monoterpene borneol, *Sci. World J.*, 2016, 7394685.
- [26] Ariyanthini, K.S., Angelina, E., Permana, K.N.B., Thelmalina, F.J., and Prasetia, I.G.N.J.A., 2021, Antibacterial activity testing of hand sanitizer gel extract of coriander (*Coriandrum sativum* L.) Seeds against *Staphylococcus aureus*, *J. Pharm. Sci. Appl.*, 3 (2), 98–107.
- [27] Razoooki, S.M.M., and Rabee, A.M., 2019, Kinetic profile of silver and zinc oxide nanoparticles by

- intraperitoneal injection in mice, a comparative study, *Period. Eng. Nat. Sci.*, 7 (3), 1499–1511.
- [28] Iciek, M., Kotańska, M., Knutelska, J., Bednarski, M., Zygmunt, M., Kowalczyk-Pachel, D., Bilaska-Wilkosz, A., Górny, M., and Sokołowska-Jeżewicz, M., 2017, The effect of NaCl on the level of reduced sulfur compounds in rat liver. Implications for blood pressure increase, *Postepy Hig. Med. Dosw.*, 71 (1), 564–576.
- [29] Wolfvoviz-Zilberman, A., Kraitman, R., Hazan, R., Friedman, M., Hourri-Haddad, Y., and Beyth, N., 2021, Phage targeting *Streptococcus mutans in vitro* and *in vivo* as a caries-preventive modality, *Antibiotics*, 10 (8), 1015.
- [30] Kono, T., Sakae, T., Nakada, H., Kaneda, T., and Okada, H., 2022, Confusion between carbonate apatite and biological apatite (carbonated hydroxyapatite) in bone and teeth, *Minerals*, 12 (2), 170.
- [31] Jeevanandam, J., Barhoum, A., Chan, Y.S., Dufresne, A., and Danquah, M.K., 2018, Review on nanoparticles and nanostructured materials: History, sources, toxicity and regulations, *Beilstein J. Nanotechnol.*, 9, 1050–1074.
- [32] Xu, Y., Chu, Y., Feng, X., Gao, C., Wu, D., Cheng, W., Meng, L., Zhang, Y., and Tang, X., 2020, Effects of zein stabilized clove essential oil Pickering emulsion on the structure and properties of chitosan-based edible films, *Int. J. Biol. Macromol.*, 156, 111–119.
- [33] da Silva, B.L., Abuçafy, M.P., Berbel Manaia, E., Oshiro Junior, J.A., Chiari-Andréo, B.G., Pietro, R.C.L.R., and Chiavacci, L.A., 2019, Relationship between structure and antimicrobial activity of zinc oxide nanoparticles: An overview, *Int. J. Nanomedicine*, 14, 9395–9410.
- [34] Liu, X., Yu, Y., Bai, X., Li, X., Zhang, J., and Wang, D., 2023, Rapid identification of insecticide- and herbicide-tolerant genetically modified maize using mid-infrared spectroscopy, *Processes*, 11 (1), 90.
- [35] Wang, M., Qian, R., Bao, M., Gu, C., and Zhu, P., 2018, Raman, FT-IR and XRD study of bovine bone mineral and carbonated apatites with different carbonate levels, *Mater. Lett.*, 210, 203–206.
- [36] Bang, L.T., Ramesh, S., Purbolaksono, J., Ching, Y.C., Long, B.D., Chandran, H., Ramesh, S., and Othman, R., 2015, Effects of silicate and carbonate substitution on the properties of hydroxyapatite prepared by aqueous co-precipitation method, *Mater. Des.*, 87, 788–796.
- [37] Mondal, S., Mondal, B., Dey, A., and Mukhopadhyay, S.S., 2012, Studies on processing and characterization of hydroxyapatite biomaterials from different bio wastes, *J. Miner. Mater. Charact. Eng.*, 11 (1), 55–67.
- [38] Cahyaningrum, S.E., Amaria, A., Ramadhan, M.I.F., and Herdyastuti, N., 2020, Synthesis hydroxyapatite/collagen/chitosan composite as bone graft for bone fracture repair, *Proceedings of the International Joint Conference on Science and Engineering (IJCSE 2020)*, Atlantis Press, Paris, France, 337–341.
- [39] Jiménez-Martínez, J., Le Borgne, T., Tabuteau, H., and Méheust, Y., 2017, Impact of saturation on dispersion and mixing in porous media: Photobleaching pulse injection experiments and shear-enhanced mixing model, *Water Resour. Res.*, 53 (2), 1457–1472.
- [40] van Dijke, K., Kobayashi, I., Schroën, K., Uemura, K., Nakajima, M., and Boom, R., 2010, Effect of viscosities of dispersed and continuous phases in microchannel oil-in-water emulsification, *Microfluid. Nanofluid.*, 9 (1), 77–85.
- [41] Chen, M.X., Alexander, K.S., and Baki, G., 2016, Formulation and evaluation of antibacterial creams and gels containing metal ions for topical application, *J. Pharm.*, 2016, 5754349.
- [42] Nugrahaeni, F., Nining, N., and Okvianida, R., 2022, The effect of HPMC concentration as a gelling agent on color stability of copigmented blush gel extract of purple sweet (*Ipomoea batatas* (L.) Lam.), *IOP Conf. Ser.: Earth Environ. Sci.*, 1041, 012070.
- [43] Bornare, S.S., Aher, S.S., and Saudagar, R.B., 2018, A review: Film forming gel novel drug delivery system, *Int. J. Curr. Pharm. Res.*, 10 (2), 25–28.
- [44] Seyedmajidi, S., Rajabnia, R., and Seyedmajidi, M., 2018, Evaluation of antibacterial properties of

- hydroxyapatite/bioactive glass and fluorapatite/bioactive glass nanocomposite foams as a cellular scaffold of bone tissue, *J. Lab. Physicians*, 10 (3), 265–270.
- [45] Subri, L.M., Dewi, W., and Satari, M.H., 2012, The antimicrobial effect of piper betel leaves extract against *Streptococcus mutans*, *Padjadjaran J. Dent.*, 24 (3), 174–178.
- [46] Nazzaro, F., Fratianni, F., De Martino, L., Coppola, R., and De Feo, V., 2013, Effect of essential oils on pathogenic bacteria, *Pharmaceuticals*, 6 (12), 1451–1474.
- [47] Lobiuc, A., Pavál, N.E., Mangalagiu, I.I., Gheorghită, R., Teliban, G.C., Amăriucăi-Mantu, D., and Stoleru, V., 2023, Future antimicrobials: Natural and functionalized phenolics, *Molecules*, 28 (3), 1114.
- [48] Xie, Y., Yang, W., Tang, F., Chen, X., and Ren, L., 2014, Antibacterial activities of flavonoids: Structure-activity relationship and mechanism, *Curr. Med. Chem.*, 22 (1), 132–149.
- [49] Yuan, G., Guan, Y., Yi, H., Lai, S., Sun, Y., and Cao, S., 2021, Antibacterial activity and mechanism of plant flavonoids to gram-positive bacteria predicted from their lipophilicities, *Sci. Rep.*, 11 (1), 10471.
- [50] Štumpf, S., Hostník, G., Primožič, M., Leitgeb, M., Salminen, J.P., and Bren, U., 2020, The effect of growth medium strength on minimum inhibitory concentrations of tannins and tannin extracts against *E. coli*, *Molecules*, 25 (12), 2947.
- [51] Kaczmarek, B., 2020, Tannic acid with antiviral and antibacterial activity as a promising component of biomaterials-A minireview, *Materials*, 13 (14), 3224.